



# Thermodynamic and kinetic interpretation of the glass-forming ability of Y-containing Cu-Zr-Al bulk metallic glasses



Mehdi Malekan<sup>a,\*</sup>, Reza Rashidi<sup>a</sup>, Saeed G. Shabestari<sup>b</sup>, Jürgen Eckert<sup>c,d,e</sup>

<sup>a</sup> School of Metallurgy and Materials Engineering, College of Engineering, University of Tehran, P.O. Box 11155-4563, Tehran, Iran

<sup>b</sup> School of Metallurgy and Materials Engineering, Iran University of Science and Technology (IUST), 16846-13114, Narmak, Tehran, Iran

<sup>c</sup> Erich Schmid Institute of Materials Science, Austrian Academy of Sciences, 8700 Leoben, Austria

<sup>d</sup> Department of Materials Science, Chair of Materials Physics, Montanuniversität Leoben, 8700 Leoben, Austria

<sup>e</sup> Adjunct with National University of Science and Technology «MISiS», Leninsky Prospekt, 4, 119049, Moscow, Russian Federation

## ARTICLE INFO

### Keywords:

Bulk metallic glasses  
Glass forming ability  
Differential scanning calorimetry  
Glass transition and crystallization  
Thermodynamic  
Kinetic

## ABSTRACT

In the present study, the glass-forming ability (GFA) of  $(\text{Cu}_{50}\text{Zr}_{43}\text{Al}_7)_{100-x}\text{Y}_x$  ( $x = 0, 2, 4$  and  $6$  at.%) bulk metallic glasses (BMGs) was investigated from thermodynamic and kinetic viewpoints. The amorphous structure of the alloys was confirmed using several techniques including X-ray diffraction (XRD), high-resolution transmission electron microscopy (HRTEM), and differential scanning calorimetry (DSC). The thermal characteristics obtained through DSC and differential thermal analysis (DTA) were employed to establish a correlation between the GFA and thermodynamics/kinetics factors. The  $(\text{Cu}_{50}\text{Zr}_{43}\text{Al}_7)_{98}\text{Y}_2$  BMG has a promising GFA of 15 mm diameter, i.e. a 50% increase in GFA compared to the base alloy. Several GFA indicators ( $\Delta T_x$ ,  $T_g$ ,  $\gamma$  and  $K$ ) confirm the excellent glass-forming capability of 2 at.% Y-doped BMG. The role of the optimum yttrium content in improving the GFA was scrutinized considering atomic, topological, and thermodynamics concepts. The interpretations imply that Y enhances the GFA through two main ways including promoting a more densely packed atomic configuration and also through scavenging oxygen as an undesirable element in glass-forming systems.

## 1. Introduction

Bulk metallic glasses (BMGs) are very popular due to their unique properties such as high strength, high elastic strain, and good corrosion and wear resistance. Among the bulk glassy alloys, Cu-based BMGs are promising for industrial applications due to relatively high strength, high thermal stability and low cost [1–3]. However, their rather low glass forming ability (GFA) limits their use in structural applications. In other words, they are limited in size in terms of dimensions. A variety of GFA indicators (for example  $\Delta T_x$  [4, 5],  $T_g$  [6],  $\gamma$  [7],  $\beta$  [7, 8],  $\omega$  [9, 10], or  $K$  [11]) have been well established and widely used in literature to make a correlation between the glass forming ability and the intrinsic features of glass formers. As such, GFA indicators explain which alloys are capable of forming glass. Taking this into consideration, these parameters can be classified into three main groups, including transformation temperature of glasses, thermodynamic models, and topological parameters. As a result, each indicator explains the GFA according to one or more of the categories listed above.

Numerous efforts have been devoted to developing BMGs with high

GFA, in various alloy systems. In order to increase the GFA, an efficient way is the minor addition of elements to the base BMG [12–20]. There are some considerations in opting proper candidates for minor addition like atomic size, mixing enthalpy, and topological effects of the added element [1]. Accordingly, rare-earth (RE) elements are promising candidates owing to their desirable features like large atomic size, significant mixing enthalpy, and oxygen adsorption tendency in regard to the base element Cu [21].

Many experimental studies have been done on the effect of minor addition of RE elements on the GFA and mechanical properties of BMGs [22–26]. It has been reported that 2 at.% addition of Gd to  $\text{Cu}_{45}\text{Zr}_{48}\text{Al}_7$  enhances the GFA [22]. Hu et al. [23] reported that the  $\text{Fe}_{66}\text{RE}_5\text{Nb}_6\text{B}_{23}$  alloy has a better GFA than the  $\text{Fe}_{71}\text{Nb}_6\text{B}_{23}$  base alloy. Zhang et al. [24] claimed that yttrium addition modifies the glass formation and melting process of the  $\text{Zr}_{55}\text{Al}_{15}\text{Ni}_{10}\text{Cu}_{20}$  alloy. Salcinovic Fetic et al. [27] produced a Cu-Zr-Al-Y glassy ribbon and examined its chemical and structural homogeneity. They reported that there is no significant difference in the chemical composition of the middle and end of the sample, which promise the reproducibility of the metallic glass.

\* Corresponding author.

E-mail address: [mmalekan@ut.ac.ir](mailto:mmalekan@ut.ac.ir) (M. Malekan).

Despite these investigations, the lack of a comprehensive thermodynamic and kinetic investigation of the role of RE elements is obvious. This insight will provide a systematic approach for the design and development of new glassy alloys. In the present work, the effect of minor addition of Y on the glass-forming ability of the  $\text{Cu}_{50}\text{Zr}_{43}\text{Al}_7$  glassy alloy was studied through both experiments and theoretical (thermodynamic and kinetic) considerations.

## 2. Materials and methods

In order to prepare alloy ingots for producing BMGs, high purity copper (99.99%), zirconium (99.9%), aluminum (99.999%), and yttrium (99.99%) with a nominal composition of  $(\text{Cu}_{50}\text{Zr}_{43}\text{Al}_7)_{100-x}\text{Y}_x$  ( $x = 0, 2, 4$  and  $6$  at.%) were mixed and arc-melted in a Ti-gettered purified argon atmosphere. The ingots were inverted and re-melted

four times to achieve chemical homogeneity. The ingots were cast into cylindrical rods with diameters ranging from  $2$  to  $16$  mm by injecting (for diameters up to  $5$  mm) and tilt casting (for diameters larger than  $5$  mm) into a copper mold in a high-vacuum chamber ( $4 \times 10^{-5}$  torr) with an argon atmosphere. The glassy and crystalline structures of the as-cast alloys were checked by X-ray diffraction (XRD, Rigaku, Cu K $\alpha$  radiation) and high-resolution transmission electron microscopy (HRTEM, JEOL 2010, 200 kV). The HRTEM samples were taken from the center of the rods, where the cooling rate is minimal. The thermal behavior of the samples was analyzed using a differential scanning calorimeter (DSC, TA DSCQ 100) at a heating rate of  $20 \text{ K min}^{-1}$ . The melting behavior of the alloys was explored by differential thermal analysis (DTA, TA SDTQ 600) through continuous heating at  $20 \text{ K min}^{-1}$ .

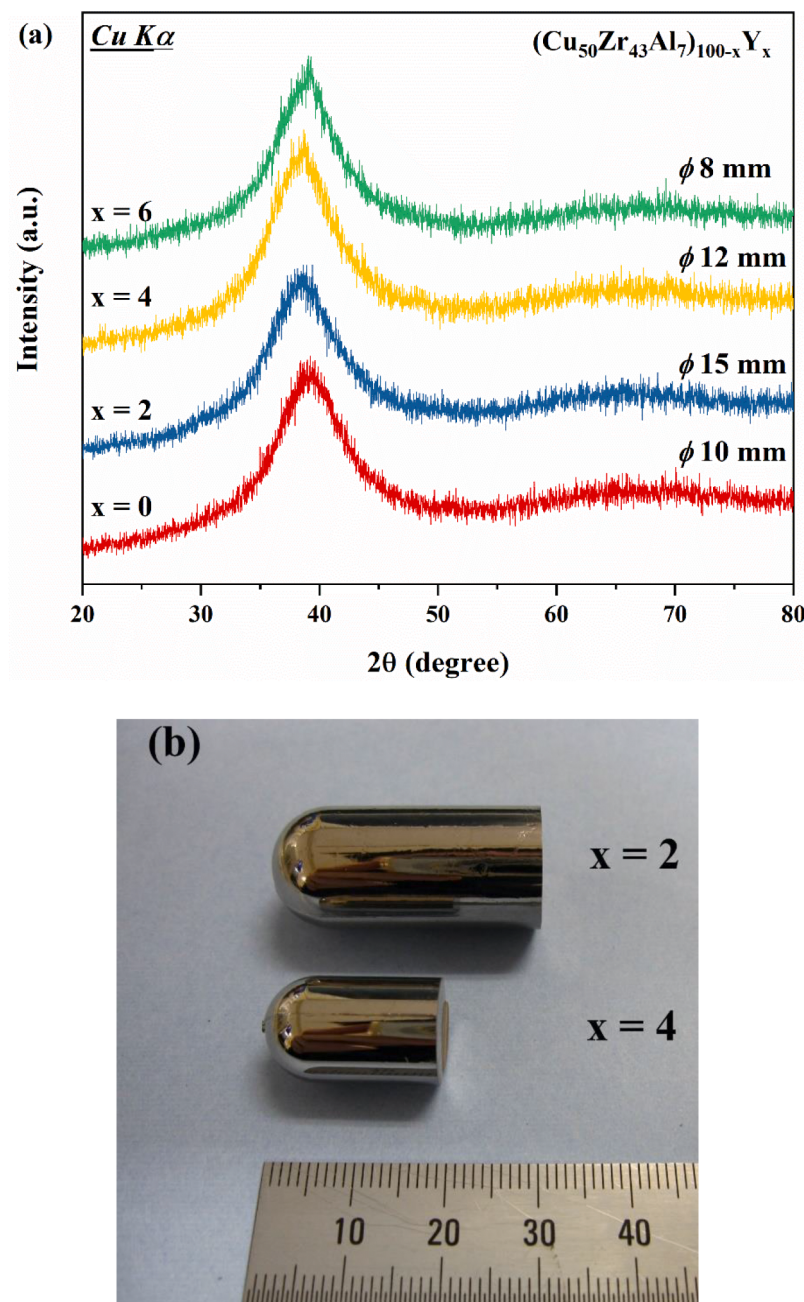


**Fig. 1.** (a) XRD patterns of as-cast  $(\text{Cu}_{50}\text{Zr}_{43}\text{Al}_7)_{100-x}\text{Y}_x$  ( $x = 0, 2, 4$  and  $6$  at.%) glassy alloys, (b) shape and outer surface appearance of  $x = 2$  with a diameter of  $15$  mm and  $x = 4$  with a diameter of  $12$  mm.

### 3. Results and discussion

The XRD patterns of the  $(\text{Cu}_{50}\text{Zr}_{43}\text{Al}_7)_{100-x}\text{Y}_x$  BMGs with their critical diameters ( $d_c$ ) are shown in Fig. 1(a). As can be seen, the XRD patterns are comprised of merely broad diffraction maxima with the first main maximum in the  $2\theta$  range of  $35^\circ - 45^\circ$  without any diffraction peaks related to crystalline phases, implying the amorphous nature of the samples. The exterior surface appearance of the as-cast  $(\text{Cu}_{50}\text{Zr}_{43}\text{Al}_7)_{98}\text{Y}_2$  and  $(\text{Cu}_{50}\text{Zr}_{43}\text{Al}_7)_{96}\text{Y}_4$  rods is shown in Fig. 1(b). Their lateral surfaces look smooth with no visible shrinkage and concaves, denoting the lack of any crystallization during the solidification of the samples. The  $\text{Cu}_{50}\text{Zr}_{43}\text{Al}_7$  base alloy has a critical diameter  $d_c$  of 10 mm, and Y doping improves the GFA of the base alloy. In this regard, the  $(\text{Cu}_{50}\text{Zr}_{43}\text{Al}_7)_{98}\text{Y}_2$  BMG with a  $d_c$  equal to 15 mm has the highest GFA compared to the other alloys of the  $(\text{Cu}_{50}\text{Zr}_{43}\text{Al}_7)_{100-x}\text{Y}_x$  system. At  $x = 4$ , the GFA increases only to 12 mm, and further addition of Y up to 6 at% reduces the GFA to 8 mm. The critical diameters ( $d_c$ ) of the glassy alloys are listed in Table 1.

Fig. 2 displays HRTEM images of as-cast samples of the  $\text{Cu}_{50}\text{Zr}_{43}\text{Al}_7$  base alloy and the 2 at.% Y doped BMG with 10 mm and 15 mm diameter, respectively. The HRTEM images show a uniform featureless microstructure, pertaining a disordered structure. The corresponding selected-area electron diffraction (SAED) patterns show diffuse halo rings, which is a typical characteristic of an amorphous structure. The results of the HRTEM images along with the XRD patterns confirm that the  $(\text{Cu}_{50}\text{Zr}_{43}\text{Al}_7)_{98}\text{Y}_2$  alloy with a diameter of 15 mm is completely amorphous and shows a remarkable and unusual GFA among the Cu-based bulk amorphous alloys. As a result, the optimum content of yttrium can efficiently suppress crystallization during the solidification of the alloy, and enhances the glass-forming ability. Nevertheless, excessive amounts of yttrium deteriorate the GFA of the alloys.

Fig. 3(a) shows the DSC curves of the  $(\text{Cu}_{50}\text{Zr}_{43}\text{Al}_7)_{100-x}\text{Y}_x$  ( $x = 0, 2, 4$  and 6 at.%) BMGs. All BMGs exhibit the same series of events including a distinct endothermic event related to the glass transition, a supercooled liquid region (SLR), and then an exothermic peak related to crystallization. The glass transition temperatures  $T_g$  and onset crystallization temperatures  $T_x$  are marked by arrows. The values of  $T_g$  and  $T_x$  are listed in Table 1.

With the increase in the yttrium content, the crystallization peaks become broader, implying more sluggish crystallization kinetics. Although  $T_g$  and  $T_x$  steadily decrease, the thermal stability of the supercooled liquid (defined as  $\Delta T_x = T_x - T_g$ ) first increases and then decreases again. The  $(\text{Cu}_{50}\text{Zr}_{43}\text{Al}_7)_{98}\text{Y}_2$  alloy has maximum thermal stability among the other Y-doped alloys, which is consistent with its maximum GFA.

Fig. 3(b) shows DTA curves related to the melting transformation of the  $(\text{Cu}_{50}\text{Zr}_{43}\text{Al}_7)_{100-x}\text{Y}_x$  ( $x = 0, 2, 4$  and 6 at.%) BMGs. The onset temperature of melting and the liquidus temperature are marked by  $T_m$  and  $T_l$ , respectively, and their values are listed in Table 1. The melting behavior of the  $(\text{Cu}_{50}\text{Zr}_{43}\text{Al}_7)_{100-x}\text{Y}_x$  glassy alloys is significantly affected by the Y content, in terms of characteristics temperatures and also the shape of the melting curve. As the Y content increases,  $T_m$  and  $T_l$  of the  $(\text{Cu}_{50}\text{Zr}_{43}\text{Al}_7)_{100-x}\text{Y}_x$  BMGs decrease from 1152 K and 1205 K for the base BMG to 1067 K and 1145 K for the 6 at.% Y-doped BMG, respectively. Although the  $\text{Cu}_{50}\text{Zr}_{43}\text{Al}_7$  base BMG is very close to the ternary eutectic composition with only one main endothermic melting event [21], it has a relatively high  $T_l$  of 1205 K. With adding 2 at.% Y,  $T_l$

of the quaternary alloy drops 1165 K. The melting transformation of  $(\text{Cu}_{50}\text{Zr}_{43}\text{Al}_7)_{98}\text{Y}_2$  consists of a small endothermic peak followed by a major endothermic event. The minor endothermic reaction can be attributed to the melting of a less-concentrated primary crystal. The two-peak melting curve implies a deviation from the eutectic composition. However, in the whole melting transformation, the fraction of the minor peak is negligible compared to the major one, and the composition of the  $(\text{Cu}_{50}\text{Zr}_{43}\text{Al}_7)_{98}\text{Y}_2$  BMG can be considered as a near-eutectic composition. Further addition of Y up to 4 and 6 at% decreases  $T_l$  to lower values of 1150 and 1145 K, respectively. In addition, the melting process transforms to a complex transformation consisting of multiple endothermic reactions, which indicates that these alloys are quaternary off-eutectic compositions. Given the highest GFA of the  $(\text{Cu}_{50}\text{Zr}_{43}\text{Al}_7)_{98}\text{Y}_2$  glassy alloy, it can be confirmed that this alloy has the closest composition to a quaternary eutectic composition among the other Y-containing alloys.

In order to evaluate the GFA of alloys, several indicators such as  $\Delta T_x = T_x - T_g$  [4, 5],  $T_{rg} = \left( \frac{T_g}{T_l} \right)$  [6],  $\gamma = \left( \frac{T_g}{T_g + T_l} \right)$  [7], or  $K = \left( \frac{T_x - T_g}{T_l - T_x} \right)$  [11] are widely used. Generally, the GFA indicators are comparative parameters, and have different ranges for the different alloy systems. However, some ideal values have been proposed for different parameters. In this regard the ideal values for the  $T_{rg}$  [6],  $\gamma$  [7, 8], and  $K$  [11] are 1, 0.5, and  $\infty$ , respectively. The higher the indicators (towards these ideal values), the better the GFA. The GFA indicator values of the  $(\text{Cu}_{50}\text{Zr}_{43}\text{Al}_7)_{100-x}\text{Y}_x$  ( $x = 0, 2, 4$  and 6 at.%) alloys are summarized in Table 1. The variation of the GFA indicators and the Y content is depicted in Fig. 4(a). A proper correlation between the calculated GFA indicators with  $d_c$  is recognized, indicating that  $\Delta T_x$ ,  $T_{rg}$ ,  $\gamma$  and  $K$  are meaningful parameters for evaluating the GFA of the  $(\text{Cu}_{50}\text{Zr}_{43}\text{Al}_7)_{100-x}\text{Y}_x$  ( $x = 0, 2, 4$  and 6 at.%) glassy alloys. For instance, the  $(\text{Cu}_{50}\text{Zr}_{43}\text{Al}_7)_{98}\text{Y}_2$  alloy with the best GFA shows the largest  $\Delta T_x$ ,  $T_{rg}$ ,  $\gamma$  and  $K$  values compared to the other alloys in the  $(\text{Cu}_{50}\text{Zr}_{43}\text{Al}_7)_{100-x}\text{Y}_x$  alloy system.

Based on Inoue's empirical criteria [5, 31], addition of proper elements is an effective way to improve the GFA of a glass-forming system. The first rule states that the alloy must consist of three or more elements. This rule supports the "confusion principle" [32] whereby the increase of the number of components makes the undercooled liquid more stable through destabilization of the competing crystalline phases. The second rule pertains to the topological viewpoint of glass formation. A significant atomic size difference between the components provides a higher atomic packing efficiency of the supercooled melt. The atomic radii of the elements are provided in Fig. 4(b). The large atomic radius of Y (1.80 Å) compared to Cu (1.28 Å), Zr (1.60 Å), and Al (1.43 Å) [29] provides a more densely packed atomic configuration. In a efficiently packed atomic structure, the diffusion and rearrangement of atoms required for phase transformation is sluggish [33]. The third principle implies that a negative mixing enthalpy among the constituent elements can facilitate glass formation. These negative values improve the atomic packing efficiency and hamper long-range diffusion of atoms through inducing the development of chemical short-range order in the liquid [4, 5]. The mixing enthalpy values of the elements with each other are presented in Fig. 4(b). In the Cu-Zr-Al-Y system, the mixing enthalpies of Cu-Zr, Cu-Al, Zr-Al, Cu-Y, Zr-Y, and Al-Y are  $-23$ ,  $-1$ ,  $-44$ ,  $-22$ ,  $0$ , and  $-31$  kJ/mol, respectively [28, 30]. It can be seen that Y addition satisfies all of Inoue's criteria.

**Table 1**

Thermal stability and GFA parameters of the  $(\text{Cu}_{50}\text{Zr}_{43}\text{Al}_7)_{100-x}\text{Y}_x$  ( $x = 0, 2, 4$  and 6 at.%) BMGs.

Composition (at%)	$T_g$ (K) ( $\pm 1$ )	$T_x$ (K) ( $\pm 1$ )	$\Delta T_x$ (K) ( $\pm 1$ )	$T_m$ (K) ( $\pm 1$ )	$T_l$ (K) ( $\pm 1$ )	$T_{rg}$	$\gamma$	$K$	$d_c$ (mm)
$\text{Cu}_{50}\text{Zr}_{43}\text{Al}_7$	717	784	67	1152	1205	0.595	0.408	0.159	10
$(\text{Cu}_{50}\text{Zr}_{43}\text{Al}_7)_{98}\text{Y}_2$	696	770	74	1072	1165	0.597	0.414	0.187	15
$(\text{Cu}_{50}\text{Zr}_{43}\text{Al}_7)_{96}\text{Y}_4$	679	715	36	1062	1150	0.590	0.391	0.083	12
$(\text{Cu}_{50}\text{Zr}_{43}\text{Al}_7)_{94}\text{Y}_6$	665	703	38	1067	1145	0.581	0.388	0.086	8

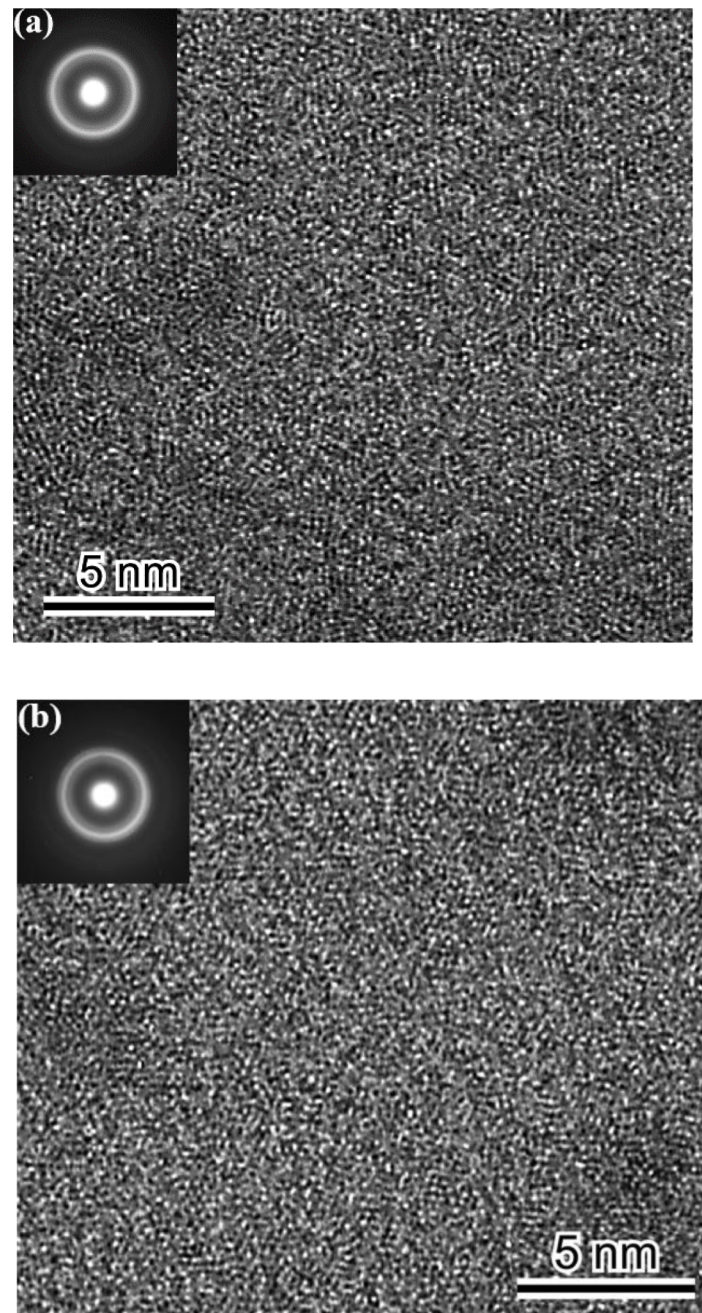


**Fig. 2.** HRTEM images and SAED patterns of as-cast (a) Cu<sub>50</sub>Zr<sub>43</sub>Al<sub>7</sub> and (b) (Cu<sub>50</sub>Zr<sub>43</sub>Al<sub>7</sub>)<sub>98</sub>Y<sub>2</sub> glassy alloys with a diameter of 10 and 15 mm, respectively.

The beneficial effect of adding yttrium in increasing the GFA is accepted in some alloy systems. However, the study of the mechanism of action of yttrium needs further investigation. It has been reported that RE elements can improve the GFA of Mg-based [34] Fe-based [35] and also Cu-based [21, 36, 37] alloys by removing oxygen impurities from the melt through the formation of harmless RE oxides. In this regard, it is valuable to investigate the role of Y in the present compositions. Considering  $\Delta G_f$  as the normalized Gibbs free energy of formation of oxide components, the concentration of dissolved oxygen [O] in the matrix regarding the equilibrium of  $xM + O \leftrightarrow M_xO$  ( $M$ : Metal; O: Oxygen) is proportional to  $\exp\left(\frac{\Delta G_f}{RT}\right)$ , given the law of mass action in thermodynamics. Furthermore, the equation of  $\Delta G_f$  can be written as follows:

$$\Delta G_f = \Delta H_f - T\Delta S_f \quad (1)$$

where,  $\Delta H_f$  and  $\Delta S_f$  are the normalized enthalpy and entropy of formation of oxide components, respectively. Therefore:

$$[O] \propto \exp\left(\frac{\Delta H_f}{RT} - \frac{\Delta S_f}{R}\right) \quad (2)$$

In the relevant temperature range (several hundred Kelvin) and the existing alloy system,  $|\frac{\Delta H_f}{RT}| \gg \frac{\Delta S_f}{R}$  [38]. According to Eq. (2), at constant temperature, [O] is strongly dependent on  $\Delta H_f$ . In other words, larger negative values of  $\Delta H_f$  would give rise to lower [O]. The  $\Delta H_f$  values for the oxide components of our alloy system including Cu<sub>2</sub>O, CuO, ZrO<sub>2</sub>, Al<sub>2</sub>O<sub>3</sub> and Y<sub>2</sub>O<sub>3</sub> are -167.47, -155.33, -1101.55, -1678.49 and -1906.67 kJ/mol [39], respectively. It can be seen that yttrium oxide (Y<sub>2</sub>O<sub>3</sub>) has the highest  $\Delta H_f$  value among all oxide components of the system, which means that the tendency for formation of Y<sub>2</sub>O<sub>3</sub> is higher than for Cu<sub>2</sub>O, CuO, ZrO<sub>2</sub>, and Al<sub>2</sub>O<sub>3</sub>. Hence, the addition of Y can reduce the oxygen

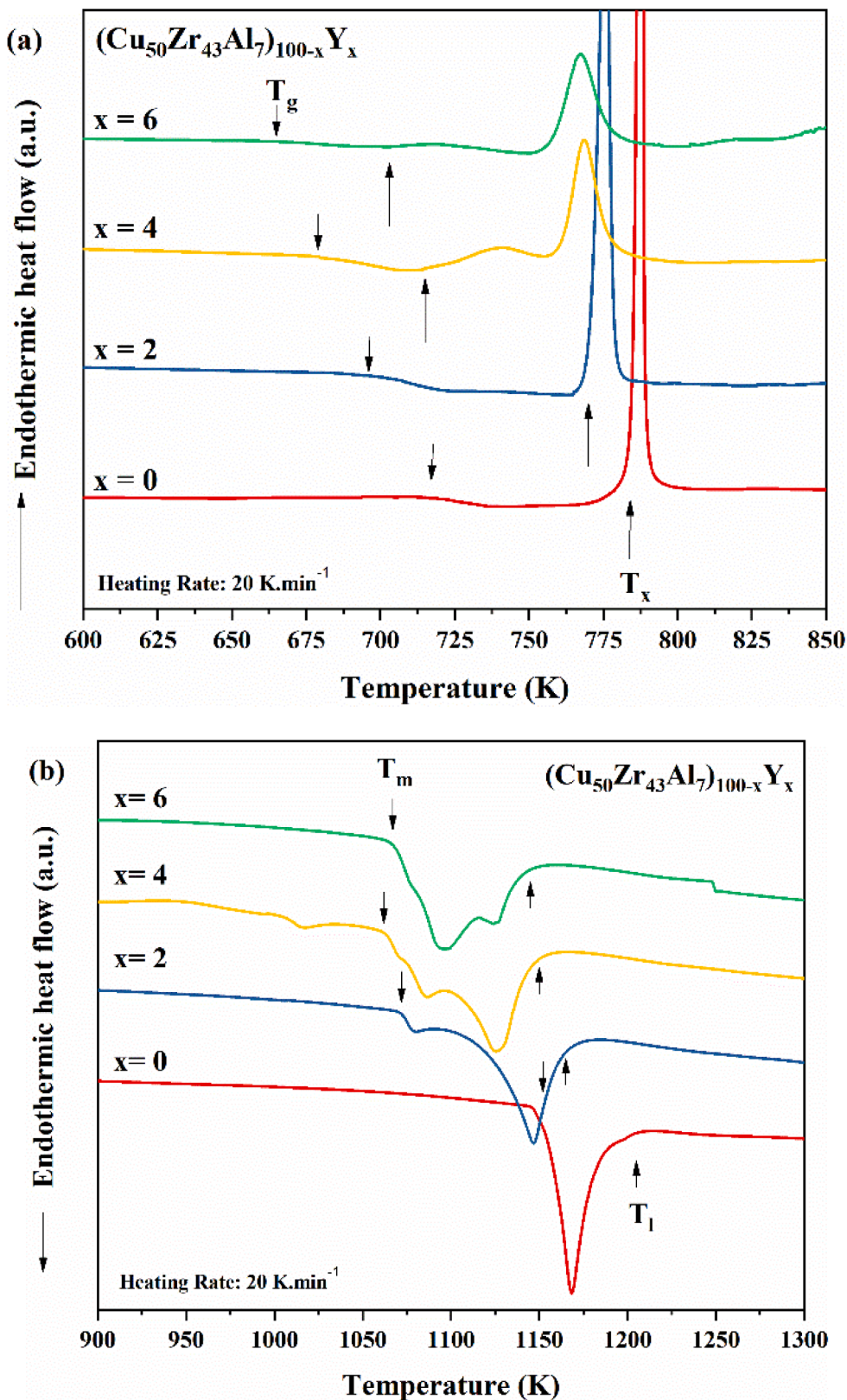
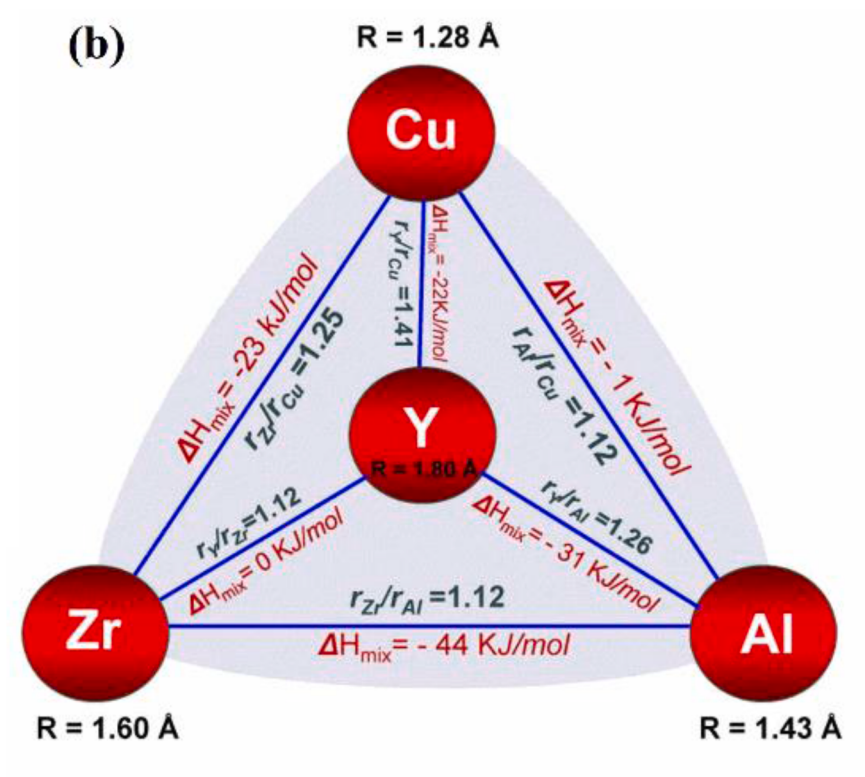
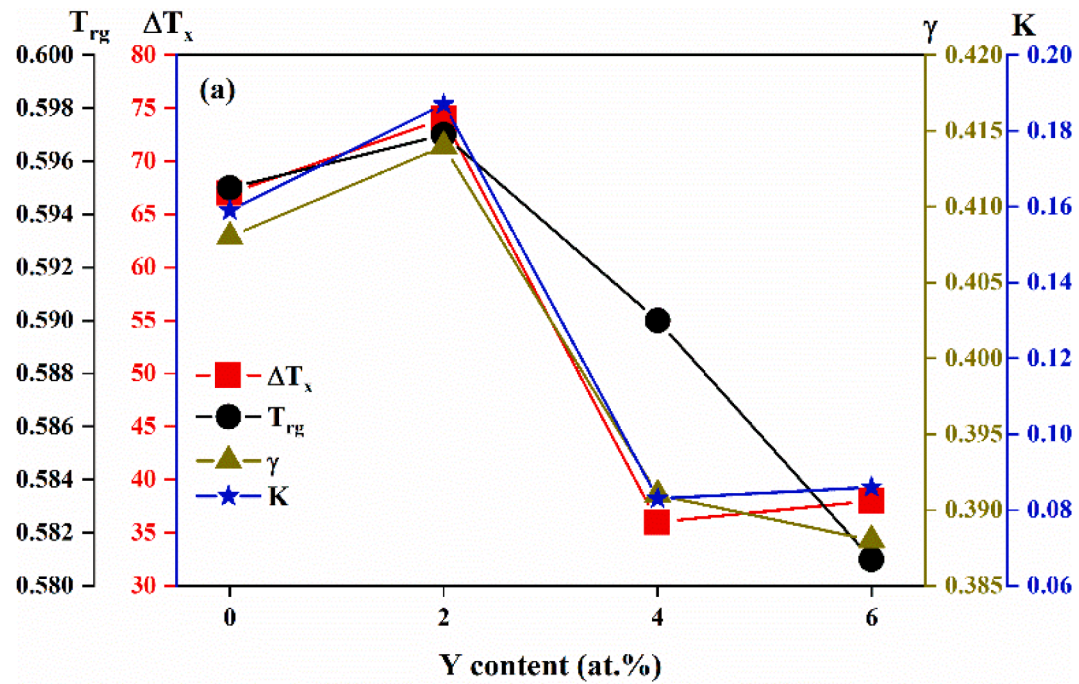


Fig. 3. (a) DSC curves ( $\text{heating rate } 20 \text{ Kmin}^{-1}$ ), and (b) DTA curves ( $\text{heating rate } 20 \text{ Kmin}^{-1}$ ) of the  $(\text{Cu}_{50}\text{Zr}_{43}\text{Al}_7)_{100-x}\text{Y}_x$  ( $x = 0, 2, 4$  and  $6$  at.%) BMGs.

concentration of the melt and also decrease the chance of formation of other oxides. Given the harmless nature of yttrium oxide [35], its formation should not promote heterogeneous nucleation of crystalline phases. Hence, it can be concluded that Y addition enhances the GFA through scavenging oxygen from the melt.

Thermodynamically, a glass-forming system with a lower driving force or higher barrier for crystallization is likely to have a better glass-forming ability [40]. The driving force for crystallization is expressed by the Gibbs free energy difference,  $\Delta G$ , between the liquid and crystalline phases. Battezzati et al. [41] suggested an equation for  $\Delta G$  in the SLR as:



**Fig. 4.** (a) Variation of GFA indicators with Y content for  $(\text{Cu}_{50}\text{Zr}_{43}\text{Al}_7)_{100-x}\text{Y}_x$  ( $x = 0, 2, 4$  and  $6$  at.%) glassy alloys, (b) mixing enthalpy between constituent elements, atomic radius size, and atomic size ratio in the Cu–Zr–Al–Y alloy system [28–30].

$$\Delta G = \frac{\Delta H_f \Delta T}{T_m} - \gamma \Delta S_f \left[ \Delta T - T \ln \left( \frac{T_m}{T} \right) \right] \quad (3)$$

where  $\Delta H_f$  is the enthalpy of fusion,  $\Delta S_f$  is the entropy of fusion ( $\Delta S_f = \frac{\Delta H_f}{T_m}$ ),  $T_m$  is the melting point,  $\Delta T$  is the undercooling ( $T_m - T$ ), and  $\gamma$  is the proportionality coefficient, which is considered to be a constant

function of the enthalpy of fusion; in the case of metallic glass-forming systems,  $\gamma$  is approximately equal to 0.8 [42].  $\Delta H_f$  can be determined through the integration of the areas under the melting peaks in the DTA curves of Fig. 3b. At  $0.8T_m$ ,  $\Delta G$  is calculated for the  $(\text{Cu}_{50}\text{Zr}_{43}\text{Al}_7)_{100-x}\text{Y}_x$  alloys. The  $\Delta H_f$  and  $\Delta G$  values are given in Table 2. As shown, the  $(\text{Cu}_{50}\text{Zr}_{43}\text{Al}_7)_{98}\text{Y}_2$  alloy exhibits the smallest  $\Delta G$  value among the

**Table 2**

Enthalpy of fusion ( $\Delta H_f$ ), Gibbs free energy difference ( $\Delta G$ ),  $T_g/(T_l - T_g)$ , and  $T_g/(T_m - T_g)$  of  $(\text{Cu}_{50}\text{Zr}_{43}\text{Al}_7)_{100-x}\text{Y}_x$  ( $x = 0, 2, 4$  and  $6$  at.%) glassy alloys.

Composition (at.%)	$\text{Cu}_{50}\text{Zr}_{43}\text{Al}_7$	$(\text{Cu}_{50}\text{Zr}_{43}\text{Al}_7)_{98}\text{Y}_2$	$(\text{Cu}_{50}\text{Zr}_{43}\text{Al}_7)_{96}\text{Y}_4$	$(\text{Cu}_{50}\text{Zr}_{43}\text{Al}_7)_{94}\text{Y}_6$
$\Delta H_f$ (J/mol)	5751.7	5604.2	6221.3	5961.8
$\Delta G$ (J/mol)	1051.4	1024.4	1137.2	1089.8
$\frac{T_g}{T_l - T_g}$	1.47	1.48	1.44	1.39
$\frac{T_g}{T_m - T_g}$	1.65	1.85	1.77	1.65

$(\text{Cu}_{50}\text{Zr}_{43}\text{Al}_7)_{100-x}\text{Y}_x$  alloys. A smaller  $\Delta G$  means a lower thermodynamic driving force for crystallization. In other words, the liquid with lower  $\Delta G$  has a larger nucleus critical size ( $r^*$ ) for nucleation. As the formation of nuclei requires diffusion, redistribution, and rearrangement of atoms, a larger  $r^*$  will require larger chemical fluctuations. This means that the  $(\text{Cu}_{50}\text{Zr}_{43}\text{Al}_7)_{98}\text{Y}_2$  alloy with lower  $\Delta G$  is more stable against crystallization, and has a better GFA.

From a kinetic point of view, it is well established that the first condition for the formation of an amorphous alloy is that the nucleation and growth rates of the crystalline phases should be sufficiently low when the molten alloy is cooled to below  $T_g$ . Based on the classical theory of nucleation and growth, the homogeneous nucleation rate ( $I$ ) and growth rate ( $U$ ) of a crystalline phase within the supercooled liquid is expressed by the following equations [1]:

$$I = \frac{10^{30}}{\eta} \cdot \exp \left( -\frac{16\pi}{3} \frac{\alpha^3 \Delta S_f T^2}{R(T_l - T)^2} \right) \quad (4)$$

$$U = \frac{10^2 f}{\eta} \cdot \left[ 1 - \exp \left( -\frac{\Delta S_f (T_l - T)}{RT} \right) \right] \quad (5)$$

Here  $\eta$  is viscosity,  $f$  is the fraction of sites at the crystal surfaces where the atomic attachment can take place.  $\alpha$  is a factor related to the atomic arrangement and the liquid/solid interfacial energy at the interface and is close to unity.  $\Delta S_f$  is the entropy of fusion,  $T$  is the liquid temperature and the  $R$  is the gas constant. As can be seen from the equations, the nucleation and growth rates of a crystalline phase at a given temperature are mainly controlled by the three parameters  $\eta$ ,  $\Delta S_f$ ,  $T/(T_l - T)$  and are inversely related to these parameters. Increasing these three parameters lowers  $I$  and  $U$ , thereby improving the GFA. For alloys that consist mainly of metallic elements,  $\Delta S_f$  does not change much from one alloy to another [4]. Hence, it can be assumed that  $\Delta S_f$  is constant. In addition, it should be noted that the effect of  $\eta$  on GFA can be evaluated from the  $T_{rg}$  and  $\Delta T_x$  values. Given that the formation of the amorphous phase occurs at  $T_g$ , and the alloy's GFA is proportional to  $I$  and  $U$ , it can be stated that:

$$\text{GFA} \propto \frac{T_g}{T_l - T_g} \quad (6)$$

Therefore, the  $T_g/(T_l - T_g)$  parameter was used as a thermal parameter to evaluate the GFA, and its values for  $(\text{Cu}_{50}\text{Zr}_{43}\text{Al}_7)_{100-x}\text{Y}_x$  glassy alloys are presented in the Table 2. As can be seen, the highest value of this parameter is for the  $(\text{Cu}_{50}\text{Zr}_{43}\text{Al}_7)_{98}\text{Y}_2$  alloy, which has the best GFA among the other alloys investigated in the present work.

#### 4. Conclusion

The optimum addition of yttrium (2 at.%) to  $\text{Cu}_{50}\text{Zr}_{43}\text{Al}_7$  BMG enhances its GFA from 10 mm to 15 mm. The  $(\text{Cu}_{50}\text{Zr}_{43}\text{Al}_7)_{98}\text{Y}_2$  BMG shows the maximum thermal stability. There is a good correlation between various GFA indicators and the critical diameter of the alloys. The  $(\text{Cu}_{50}\text{Zr}_{43}\text{Al}_7)_{98}\text{Y}_2$  BMG exhibits minimum thermodynamic driving force for crystallization, which implies its greater resistance against crystallization in the undercooled liquid state, and higher GFA. The proper amount of yttrium plays an effective role in enhancing the GFA of the BMG system. Yttrium affects the GFA through two main ways: (i) enhancing the atomic packing configuration, and (ii) scavenging oxygen

and formation of harmless oxides. Several thermodynamic and kinetic factors confirm the effective role of the optimum content of yttrium on the GFA.

#### CRediT authorship contribution statement

**Mehdi Malekan:** Conceptualization, Methodology, Formal analysis, Investigation, Writing – review & editing, Supervision, Project administration. **Reza Rashidi:** Methodology, Formal analysis, Investigation, Writing – original draft. **Saeed G. Shabestari:** Conceptualization, Methodology, Formal analysis, Supervision. **Jürgen Eckert:** Methodology, Formal analysis, Writing – review & editing.

#### Declaration of Competing Interest

The authors declare that they have no known competing financial interests or personal relationships that could have appeared to influence the work reported in this paper.

#### References

- [1] C. Suryanarayana, A. Inoue, Bulk Metallic Glasses, CRC press, 2017.
- [2] J.F. Löfller, Bulk metallic glasses, *Intermetallics* 11 (2003) 529–540.
- [3] J. Eckert, J. Das, S. Pauly, C. Duhamel, Mechanical properties of bulk metallic glasses and composites, *J. Mater. Res.* 22 (2007) 285–301.
- [4] A. Inoue, Bulk Amorphous Alloys, Trans Tech Publications, Uetikon-Zuerich Switzerland, 1999.
- [5] A. Inoue, Stabilization of metallic supercooled liquid and bulk amorphous alloys, *Acta Mater.* 48 (2000) 279–306.
- [6] D. Turnbull, Under what conditions can a glass be formed? *Contemp. Phys.* 10 (1969) 473–488.
- [7] Z. Lu, C. Liu, A new glass-forming ability criterion for bulk metallic glasses, *Acta Mater.* 50 (2002) 3501–3512.
- [8] Z. Lu, C. Liu, Glass formation criterion for various glass-forming systems, *Phys. Rev. Lett.* 91 (2003), 115505.
- [9] Z. Long, H. Wei, Y. Ding, P. Zhang, G. Xie, A. Inoue, A new criterion for predicting the glass-forming ability of bulk metallic glasses, *J. Alloys Compd.* 475 (2009) 207–219.
- [10] Z. Long, G. Xie, H. Wei, X. Su, J. Peng, P. Zhang, A. Inoue, On the new criterion to assess the glass-forming ability of metallic alloys, *Mater. Sci. Eng.: A* 509 (2009) 23–30.
- [11] A. Hrubý, Evaluation of glass-forming tendency by means of DTA, *Czechoslovak J. Phys. B* 22 (1972) 1187–1193.
- [12] Z.P. Lu, C.T. Liu, Role of minor alloying additions in formation of bulk metallic glasses: a Review, *J. Mater. Sci.* 39 (2004) 3965–3974.
- [13] R. Rashidi, M. Malekan, R. Gholamipour, Microstructure and mechanical properties of a Cu-Zr based bulk metallic glass containing atomic scale chemical heterogeneities, *Mater. Sci. Eng.: A* 729 (2018) 433–438.
- [14] S. González, Role of minor additions on metallic glasses and composites, *J. Mater. Res.* 31 (2015) 76–87.
- [15] Y.D. Sun, Q.R. Chen, G.Z. Li, Enhanced glass forming ability and plasticity of Mg-based bulk metallic glass by minor addition of Cd, *J. Alloys Compd.* 584 (2014) 273–278.
- [16] C.T. Liu, Z.P. Lu, Effect of minor alloying additions on glass formation in bulk metallic glasses, *Intermetallics* 13 (2005) 415–418.
- [17] S. Bera, P. Ramasamy, D. Şopu, B. Sarac, J. Zálesák, C. Gammer, M. Stoica, M. Calin, J. Eckert, Tuning the glass forming ability and mechanical properties of Ti-based bulk metallic glasses by Ga additions, *J. Alloys Compd.* 793 (2019) 552–563.
- [18] J.-L. Gu, Y. Shao, S.-F. Zhao, S.-Y. Lu, G.-N. Yang, S.-Q. Chen, K.-F. Yao, Effects of Cu addition on the glass forming ability and corrosion resistance of Ti-Zr-Be-Ni alloys, *J. Alloys Compd.* 725 (2017) 573–579.
- [19] M. Samavatian, R. Gholamipour, V. Samavatian, F. Farahani, Effects of Nb minor addition on atomic structure and glass forming ability of Zr55Cu30Ni5Al10 bulk metallic glass, *Mater. Res. Express* 6 (2019), 065202.
- [20] M. Malekan, R. Rashidi, Effective role of minor silicon addition on crystallization kinetics of  $\text{Cu}_{50}\text{Zr}_{43}\text{Al}_7$  bulk metallic glass, *Appl. Phys. A* 127 (2021) 246.

- [21] M. Malekan, R. Rashidi, S.G. Shabestari, Mechanical properties and crystallization kinetics of Er-containing Cu-Zr-Al bulk metallic glasses with excellent glass forming ability, Vacuum 174 (2020), 109223.
- [22] X. Xu, L.Y. Chen, G.Q. Zhang, L.N. Wang, J.Z. Jiang, Formation of bulk metallic glasses in Cu45Zr48-xAl7REx (RE=La, Ce, Nd, Gd and 0≤x≤5at.%), Intermetallics 15 (2007) 1066–1070.
- [23] F. Hu, C. Yuan, Q. Luo, W. Yang, B. Shen, Effects of heavy rare-earth addition on glass-forming ability, thermal, magnetic, and mechanical properties of Fe-RE-B-Nb (RE = Dy, Ho, Er or Tm) bulk metallic glass, J. Non Cryst. Solids 525 (2019), 119681.
- [24] Y. Zhang, M.X. Pan, D.Q. Zhao, R.J. Wang, W.H. Wang, Formation of Zr-Based Bulk Metallic Glasses from Low Purity of Materials by Yttrium Addition, Mater. Trans. JIM 41 (2000) 1410–1414.
- [25] F. Hu, C. Yuan, Q. Luo, W. Yang, B. Shen, Effects of heavy rare-earth addition on glass-forming ability, thermal, magnetic, and mechanical properties of Fe-RE-B-Nb (RE= Dy, Ho, Er or Tm) bulk metallic glass, J. Non Cryst. Solids 525 (2019), 119681.
- [26] L. Deng, B. Zhou, H. Yang, X. Jiang, B. Jiang, X. Zhang, Roles of minor rare-earth elements addition in formation and properties of Cu-Zr-Al bulk metallic glasses, J. Alloys Compd. 632 (2015) 429–434.
- [27] A.S. Fetić, A. Selimović, B. Fakić, K. Hrvat, M. Djekić, Homogeneity and structure of CuZrAlY metallic glass ribbons, AIP Conf. Proc. 1722 (2016), 220023.
- [28] A. Takeuchi, A. Inoue, Classification of bulk metallic glasses by atomic size difference, heat of mixing and period of constituent elements and its application to characterization of the main alloying element, Mater. Trans. 46 (2005) 2817–2829.
- [29] O. Senkov, D. Miracle, Effect of the atomic size distribution on glass forming ability of amorphous metallic alloys, Mater. Res. Bull. 36 (2001) 2183–2198.
- [30] F.J.A.e.N.-H. De Boer, Cohesion in metals. Transition metal alloys/FR de Boer, R. Boom, WCM Mattens, AR Miedema et al., (1988).
- [31] Q. An, K. Samwer, M.D. Demetriou, M.C. Floyd, D.O. Duggins, W.L. Johnson, W. A. Goddard 3rd, How the toughness in metallic glasses depends on topological and chemical heterogeneity, Proc. Natl. Acad. Sci. U. S. A. 113 (2016) 7053–7058.
- [32] A.L. Greer, Confusion by design, Nature 366 (1993) 303–304.
- [33] D. Xu, G. Duan, W.L. Johnson, Unusual Glass-Forming Ability of Bulk Amorphous Alloys Based on Ordinary Metal Copper, Phys. Rev. Lett. 92 (2004), 245504.
- [34] X. Xi, R. Wang, D. Zhao, M. Pan, W. Wang, Glass-forming Mg–Cu–RE (RE= Gd, Pr, Nd, Tb, Y, and Dy) alloys with strong oxygen resistance in manufacturability, J. Non Cryst. Solids 344 (2004) 105–109.
- [35] Z. Lu, C. Liu, W. Porter, Role of yttrium in glass formation of Fe-based bulk metallic glasses, Appl. Phys. Lett. 83 (2003) 2581–2583.
- [36] H. Fu, H. Wang, H. Zhang, Z. Hu, The effect of Gd addition on the glass-forming ability of Cu-Zr-Al alloy, Scr. Mater. 55 (2006) 147–150.
- [37] X. Xu, L. Chen, G. Zhang, L. Wang, J. Jiang, Formation of bulk metallic glasses in Cu45Zr48-xAl7REx (RE= La, Ce, Nd, Gd and 0≤ x≤ 5 at.%), Intermetallics 15 (2007) 1066–1070.
- [38] D. Xu, Development of Novel Binary and Multi-Component Bulk Metallic Glasses, in: California Institute of Technology, 2005.
- [39] L. Pankratz, Thermodynamic Properties of Elements and oxides, US Department of the Interior, Bureau of Mines, 1982.
- [40] R. Busch, Y. Kim, W. Johnson, Thermodynamics and kinetics of the undercooled liquid and the glass transition of the Zr41. 2Ti13. 8Cu12. 5Ni10. 0Be22. 5 alloy, J. Appl. Phys. 77 (1995) 4039–4043.
- [41] L. Battezzati, E. Garrone, On the approximation of the free energy of undercooled glass-forming metallic melts, Zeitschrift Für Metallkunde 75 (1984) 305–310.
- [42] F. Guo, S.J. Poon, G.J. Shiflet, Metallic glass ingots based on yttrium, Appl. Phys. Lett. 83 (2003) 2575–2577.